

Exact Rheology of Uniform Shear Flow in a Gas of Inelastic and Rough Maxwell Particles

Andrés Santos^{1*} and Gilberto M. Kremer²

¹Departamento de Física and Instituto de Computación Científica Avanzada (ICCAEx), Universidad de Extremadura, Badajoz, E-06006, Spain.

²Departamento de Física, Universidade Federal do Paraná, Curitiba, Brazil.

*Corresponding author(s). E-mail(s): andres@unex.es;
Contributing authors: kremer@fisica.ufpr.br;

Abstract

We investigate the steady uniform shear flow of a granular gas composed of inelastic and rough Maxwell particles. Exploiting the mean-field character of the model, we derive exact expressions for the collisional production rates of the second-degree moments and obtain a closed nonlinear solution for the stress and spin-spin tensors. The rotational-to-translational temperature ratio and the proportionality between the spin-spin and stress tensors are shown to be independent of the coefficient of normal restitution and determined solely by roughness and moment of inertia. The reduced normal stresses, shear stress, and shear rate are obtained explicitly in terms of two effective parameters generalizing the cooling and stress relaxation rates of the smooth model. From these results we derive exact expressions for the non-Newtonian shear viscosity, the first viscometric function, and the friction coefficient. The dependence of the rheological properties on the normal and tangential restitution coefficients is analyzed in detail, revealing strong non-Newtonian behavior and nonmonotonic effects of roughness. The results reduce, in the appropriate limits, to those of the inelastic Maxwell model for smooth particles and to the Pidduck gas in the elastic perfectly rough case.

Keywords: Granular gas; Inelastic collisions; Rough particles; Maxwell model; Uniform shear flow

1 Introduction

The most widely used model for a granular gas is the inelastic hard-sphere model (IHSM), where the grains are assumed to be perfectly smooth spheres colliding with a constant coefficient of normal restitution α [1, 2]. A much more tractable alternative is the inelastic Maxwell model (IMM), in which the velocity-dependent collision rate is replaced by an effective mean-field constant [3]. This simplification has been widely exploited to obtain a variety of exact results within the IMM framework. However, both the IHSM and the IMM neglect the impact of surface roughness on the dynamical properties of granular gases. This limitation is overcome by the inelastic rough hard-sphere model (IRHSM), where, in addition to α , a constant coefficient of tangential restitution β is introduced [4].

In parallel with the simplification leading from the IHSM to the IMM, we have recently proposed the inelastic rough Maxwell model (IRMM) as a Maxwellian counterpart of the IRHSM. In a first work, we derived the exact expressions for the most relevant collisional moments [5], and in a second one we obtained the exact Navier–Stokes–Fourier (NSF) transport coefficients [6].

It is well known that nonequilibrium steady states of granular gases are inherently non-Newtonian, so that the stress tensor Π_{ij} may significantly deviate from its NSF form [2, 7]. From a theoretical viewpoint, the paradigmatic nonequilibrium state is the uniform (or simple) shear flow (USF). This state is characterized by a constant shear rate $\dot{\gamma}$ and a spatially uniform velocity distribution function in the Lagrangian frame, $f(\mathbf{V})$, where $\mathbf{V} = \mathbf{v} - \dot{\gamma}y\mathbf{e}_x$ is the peculiar velocity.

The USF for the IHSM has been extensively studied by means of computer simulations [8–14], kinetic models [15–17], and approximate solutions of the Boltzmann and Enskog equations, such as Grad’s moment method [7, 12–14, 18, 19]. In the case of the IMM, the velocity-independence of the collision rate allows for the derivation of exact results [16, 17, 20–33].

The inclusion of roughness in the IRHSM renders the model more realistic but also considerably increases its mathematical complexity. In analogy with the IHSM, the USF for the IRHSM has been investigated by computer simulations [34], kinetic modeling [35, 36], and Grad’s moment method [36].

The aim of the present work is to complement the previous studies on the non-Newtonian rheological properties of the USF by deriving exact results within the framework of the IRMM.

The paper is organized as follows. In Sect. 2 we formulate the Boltzmann equation for the steady uniform shear flow and derive the hierarchy of balance equations for the relevant velocity moments. Section 3 recalls the definition of the IRMM and the exact expressions of the collisional production rates needed for the USF problem. In Sect. 4 we obtain the exact solution for the reduced stress and spin-spin tensors, analyze the resulting nonlinear rheological properties, and discuss their dependence on the coefficients of restitution and the moment of inertia. The main conclusions are summarized in Sect. 5.

2 Boltzmann equation for the uniform shear flow

2.1 Collision rules

Let us consider a granular gas composed of spherical particles of diameter σ , mass m , and moment of inertia I . The translational and angular velocities of a particle are denoted by \mathbf{v} and $\boldsymbol{\omega}$, respectively.

In both the IRHSM and the IRMM, collisions are characterized by a constant coefficient of normal restitution α and a constant coefficient of tangential restitution β . If $(\mathbf{v}_1, \boldsymbol{\omega}_1; \mathbf{v}_2, \boldsymbol{\omega}_2)$ are the precollisional velocities of a colliding pair, the corresponding postcollisional velocities are given by [2, 37]

$$\hat{b}_{\hat{\boldsymbol{\sigma}}} \begin{Bmatrix} \mathbf{v}_1 \\ \mathbf{v}_2 \end{Bmatrix} = \begin{Bmatrix} \mathbf{v}_1 \\ \mathbf{v}_2 \end{Bmatrix} \mp \frac{\mathbf{Q}}{m}, \quad \hat{b}_{\hat{\boldsymbol{\sigma}}} \begin{Bmatrix} \boldsymbol{\omega}_1 \\ \boldsymbol{\omega}_2 \end{Bmatrix} = \begin{Bmatrix} \boldsymbol{\omega}_1 \\ \boldsymbol{\omega}_2 \end{Bmatrix} - \frac{\sigma}{2} \hat{\boldsymbol{\sigma}} \times \frac{\mathbf{Q}}{I}, \quad (1)$$

where $\hat{b}_{\hat{\boldsymbol{\sigma}}}$ is the collision operator in velocity space, $\hat{\boldsymbol{\sigma}}$ is the unit vector joining the centers of the two colliding particles at contact, and \mathbf{Q} is the impulse exerted by particle 1 on particle 2. Its explicit expression is

$$\mathbf{Q} = m\tilde{\alpha}(\hat{\boldsymbol{\sigma}} \cdot \mathbf{g})\hat{\boldsymbol{\sigma}} - m\tilde{\beta}\hat{\boldsymbol{\sigma}} \times \left(\hat{\boldsymbol{\sigma}} \times \mathbf{g} + \sigma \frac{\boldsymbol{\omega}_1 + \boldsymbol{\omega}_2}{2} \right), \quad (2)$$

where $\mathbf{g} = \mathbf{v}_1 - \mathbf{v}_2$ is the relative translational velocity of the centers of mass. The parameters

$$\tilde{\alpha} \equiv \frac{1 + \alpha}{2}, \quad \tilde{\beta} \equiv \frac{1 + \beta}{2} \frac{\kappa}{1 + \kappa}, \quad \kappa \equiv \frac{I}{m\sigma^2}, \quad (3)$$

are functions of the coefficients of restitution and of the reduced moment of inertia κ .

2.2 Boltzmann equation

In the special case of the steady-state USF, the Boltzmann equation takes the form

$$-\dot{\gamma} V_y \frac{\partial f(\mathbf{V}, \boldsymbol{\omega})}{\partial V_x} = J[\mathbf{V}, \boldsymbol{\omega} | f, f], \quad (4)$$

where $\dot{\gamma}$ is the constant shear rate, $f(\mathbf{V}, \boldsymbol{\omega})$ is the spatially uniform velocity distribution function in the Lagrangian frame, and $\mathbf{V} = \mathbf{v} - \dot{\gamma} y \mathbf{e}_x$ is the peculiar velocity. The left-hand side of Eq. (4) accounts for the effect of the shear field in the co-moving frame, while the right-hand side represents the Boltzmann bilinear collision operator.

4 Rheology of Uniform Shear Flow

Given an arbitrary function $\Psi(\mathbf{V}, \boldsymbol{\omega})$, we define its average value $\langle \Psi \rangle$ and its collisional production rate $\mathcal{J}[\Psi]$ as

$$\langle \Psi \rangle = \frac{1}{n} \int d\mathbf{V} \int d\boldsymbol{\omega} \Psi(\mathbf{V}, \boldsymbol{\omega}) f(\mathbf{V}, \boldsymbol{\omega}), \quad (5a)$$

$$\mathcal{J}[\Psi] = \frac{1}{n} \int d\mathbf{V} \int d\boldsymbol{\omega} \Psi(\mathbf{V}, \boldsymbol{\omega}) J[\mathbf{V}, \boldsymbol{\omega} | f, f], \quad (5b)$$

where n is the number density. By definition and conservation of linear momentum, one has $\langle \mathbf{V} \rangle = \mathcal{J}[\mathbf{V}] = 0$.

In the USF problem, the most relevant quantities are the first- and second-degree velocity moments:

$$\boldsymbol{\Omega} = \langle \boldsymbol{\omega} \rangle, \quad \Upsilon_{ij} = n \langle \omega_i V_j \rangle, \quad (6a)$$

$$T_t = \frac{m}{3} \langle V^2 \rangle, \quad T_r = \frac{I}{3} \langle \omega^2 \rangle, \quad (6b)$$

$$\Pi_{ij} = nm \left\langle V_i V_j - \frac{1}{3} V^2 \delta_{ij} \right\rangle, \quad \Omega_{ij} = nI \left\langle \omega_i \omega_j - \frac{1}{3} \omega^2 \delta_{ij} \right\rangle. \quad (6c)$$

Here, $\boldsymbol{\Omega}$ is the mean spin vector, Υ_{ij} is the couple stress tensor [38, 39], T_t and T_r are the translational and rotational granular temperatures, respectively, Π_{ij} is the (traceless) stress tensor, and Ω_{ij} is the (traceless) spin-spin tensor. Note that the pressure tensor is

$$P_{ij} = nm \langle V_i V_j \rangle = \Pi_{ij} + nT_t \delta_{ij}. \quad (7)$$

Taking moments on both sides of Eq. (4), one straightforwardly obtains the following balance equations:

$$\mathcal{J}[\boldsymbol{\omega}] = 0, \quad n\mathcal{J}[\omega_i V_j] = \dot{\gamma} \Upsilon_{iy} \delta_{jx}, \quad (8a)$$

$$nm\mathcal{J}[V^2] = 2\dot{\gamma}\Pi_{xy}, \quad \mathcal{J}[\omega^2] = 0, \quad \mathcal{J} \left[\omega_i \omega_j - \frac{1}{3} \omega^2 \delta_{ij} \right] = 0, \quad (8b)$$

$$\begin{aligned} nm\mathcal{J} \left[V_i V_j - \frac{1}{3} V^2 \delta_{ij} \right] = & \dot{\gamma} \left[\Pi_{iy} \delta_{jx} + \Pi_{jy} \delta_{ix} - \frac{2}{3} \Pi_{xy} \delta_{ij} \right. \\ & \left. + nT_t (\delta_{ix} \delta_{jy} + \delta_{iy} \delta_{jx}) \right]. \end{aligned} \quad (8c)$$

Within the IRHSM, the production rates $\mathcal{J}[\Psi]$ cannot, in general, be evaluated exactly. This limitation is overcome in the IRMM, where the mean-field character of the collision rate allows one to obtain closed expressions for those collisional moments.

3 The inelastic and rough Maxwell model

In the IRMM, the Boltzmann collision operator is given by [5, 6]

$$J[\mathbf{V}_1, \boldsymbol{\omega}_1 | f, f] = \frac{\nu}{4\pi n} \int d\mathbf{V}_2 \int d\boldsymbol{\omega}_2 \int d\hat{\boldsymbol{\sigma}} \left(\frac{\hat{b}_{\hat{\boldsymbol{\sigma}}}^{-1}}{\alpha\beta^2} - 1 \right) f(\mathbf{V}_1, \boldsymbol{\omega}_1) f(\mathbf{V}_2, \boldsymbol{\omega}_2), \quad (9)$$

where $\nu \propto \sqrt{T_t}$ is an effective mean-field collision frequency.

The mean-field structure of Eq. (9) allows one to evaluate exactly the production rates appearing in Eqs. (13c) [5]. In particular,

$$-\nu^{-1} \mathcal{J}[\boldsymbol{\omega}] = \varphi_{01|01} \boldsymbol{\Omega}, \quad -\nu^{-1} n \mathcal{J}[\omega_i V_j] = \psi_{11|11} \Upsilon_{ij}, \quad (10)$$

where the coefficients $\varphi_{01|01}$ and $\psi_{11|11}$ depend on α , β , and κ , although their explicit expressions are not required here. Substitution of Eq. (10) into Eq. (8a) implies that $\boldsymbol{\Omega} = \Upsilon_{ij} = 0$ in the USF state.

Under this condition, the production rates associated with Eqs. (8b) and (8c) become

$$-\nu^{-1} \frac{m}{3} \mathcal{J}[V^2] = \chi_{20|20} T_t + \frac{4}{\kappa} \chi_{20|02} T_r, \quad (11a)$$

$$-\nu^{-1} \frac{I}{3} \mathcal{J}[\omega^2] = \frac{\kappa}{4} \chi_{02|20} T_t + \chi_{02|02} T_r, \quad (11b)$$

$$-\nu^{-1} nm \mathcal{J}\left[V_i V_j - \frac{1}{3} V^2 \delta_{ij}\right] = \psi_{20|20} \Pi_{ij} + \frac{4}{\kappa} \psi_{20|02} \Omega_{ij}, \quad (11c)$$

$$-\nu^{-1} nI \mathcal{J}\left[\omega_i \omega_j - \frac{1}{3} \omega^2 \delta_{ij}\right] = \frac{\kappa}{4} \psi_{02|20} \Pi_{ij} + \psi_{02|02} \Omega_{ij}. \quad (11d)$$

The explicit expressions of the eight coefficients appearing in Eqs. (11) are [5]

$$\chi_{20|20} = \frac{2}{3} \left[\tilde{\alpha} (1 - \tilde{\alpha}) + 2\tilde{\beta} (1 - \tilde{\beta}) \right], \quad \chi_{20|02} = -\frac{\tilde{\beta}^2}{3}, \quad (12a)$$

$$\chi_{02|20} = -\frac{16\tilde{\beta}^2}{3\kappa^2}, \quad \chi_{02|02} = \frac{4\tilde{\beta}}{3\kappa} \left(1 - \frac{\tilde{\beta}}{\kappa} \right), \quad (12b)$$

$$\psi_{20|20} = \frac{2}{15} \left(5\tilde{\alpha} - 2\tilde{\alpha}^2 - 6\tilde{\alpha}\tilde{\beta} + 10\tilde{\beta} - 7\tilde{\beta}^2 \right), \quad (12c)$$

$$\psi_{20|02} = \frac{\tilde{\beta}^2}{6}, \quad \psi_{02|20} = \frac{8\tilde{\beta}^2}{3\kappa^2}, \quad \psi_{02|02} = \frac{2\tilde{\beta}}{15\kappa} \left(10 - \frac{7\tilde{\beta}}{\kappa} \right). \quad (12d)$$

4 Results

Insertion of Eqs. (11) into Eqs. (8b) and (8c) yields

$$\theta \equiv \frac{T_r}{T_t} = -\frac{\kappa}{4} \frac{\chi_{02|20}}{\chi_{02|02}} = \frac{\kappa(1 + \beta)}{1 - \beta + 2\kappa}, \quad (13a)$$

6 Rheology of Uniform Shear Flow

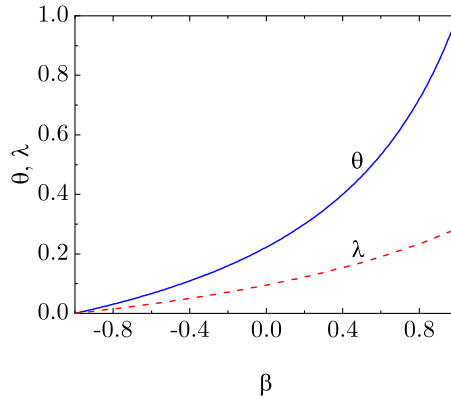


Fig. 1 Rotational-to-translational temperature ratio $\theta = T_r/T_t$ and proportionality factor λ relating the spin-spin tensor to the stress tensor, $\Omega_{ij}^* = -\lambda\Pi_{ij}^*$, as functions of the tangential restitution coefficient β for $\kappa = \frac{2}{5}$.

$$\chi_{20|20} + \frac{4}{\kappa}\chi_{20|02}\theta = -\frac{2}{3}\dot{\gamma}^*\Pi_{xy}^*, \quad (13b)$$

$$\psi_{20|20}\Pi_{ij}^* + \frac{4}{\kappa}\psi_{20|02}\Omega_{ij}^* = \dot{\gamma}^* \left(\frac{2}{3}\Pi_{xy}^*\delta_{ij} - \Pi_{iy}^*\delta_{jx} - \Pi_{jy}^*\delta_{ix} - \delta_{ix}\delta_{jy} - \delta_{jx}\delta_{iy} \right), \quad (13c)$$

$$\Omega_{ij}^* = -\lambda\Pi_{ij}^*, \quad \lambda = \frac{\kappa\psi_{02|20}}{4\psi_{02|02}} = \frac{5\kappa(1+\beta)}{13-7\beta+20\kappa}, \quad (13d)$$

where $\dot{\gamma}^* \equiv \dot{\gamma}/\nu$ is the reduced shear rate, $\Pi_{ij}^* \equiv \Pi_{ij}/nT_t$ is the reduced stress tensor, and $\Omega_{ij}^* \equiv \Omega_{ij}/nT_t$ is the reduced spin-spin tensor.

Equation (13a) shows that the rotational-to-translational temperature ratio θ is independent of the coefficient of normal restitution α . It ranges from $\theta = 0$ in the perfectly smooth case ($\beta = -1$) to $\theta = 1$ in the perfectly rough case ($\beta = 1$). This temperature ratio coincides with that obtained from a Bhatnagar–Gross–Krook-like model [35] and also with the one corresponding to the homogeneous steady state driven by a white-noise thermostat. Moreover, according to Eq. (13d), the spin-spin tensor is proportional to the stress tensor, $\Omega_{ij}^* = -\lambda\Pi_{ij}^*$, with a negative proportionality factor $-\lambda$ that is independent of α and vanishes in the perfectly smooth limit ($\beta = -1$). Figure 1 displays the β -dependence of both θ and λ for $\kappa = \frac{2}{5}$.

Substitution of Eq. (13a) into Eq. (13b) gives

$$\frac{2}{3}\dot{\gamma}^*\Pi_{xy}^* = -\chi, \quad (14)$$

where

$$\chi \equiv \chi_{20|20} - \frac{\chi_{20|02}\chi_{02|20}}{\chi_{02|02}} = \frac{2}{3} \left(\frac{1-\alpha^2}{4} + \kappa \frac{1-\beta^2}{1-\beta+2\kappa} \right) \quad (15)$$

is proportional to the translational cooling rate. Likewise, insertion of Eq. (13d) into Eq. (13c) yields

$$\dot{\gamma}^* \left(\frac{2}{3} \Pi_{xy}^* \delta_{ij} - \Pi_{iy}^* \delta_{jx} - \Pi_{jy}^* \delta_{ix} - \delta_{ix} \delta_{jy} - \delta_{jx} \delta_{iy} \right) = \psi \Pi_{ij}^*, \quad (16)$$

where

$$\psi \equiv \psi_{20|20} - \frac{\psi_{20|02} \psi_{02|20}}{\psi_{02|02}} = \frac{1+\alpha}{3} - \frac{(1+\alpha)^2}{15} + \frac{\kappa(1+\beta)}{1+\kappa} \left[\frac{2}{3} - \frac{1+\alpha}{5} - \frac{7\kappa(1+\beta)}{30(1+\kappa)} - \frac{5\kappa(1+\beta)^2}{6(1+\kappa)(13-7\beta+20\kappa)} \right] \quad (17)$$

can be interpreted as the stress relaxation rate.

The structure of Eqs. (14) and (16) is the same as in the smooth case [23]. The solution is $\Pi_{xz}^* = \Pi_{yz}^* = 0$ and

$$\Pi_{xx}^* = -2\Pi_{yy}^* = -2\Pi_{zz}^* = 2\frac{\chi}{\psi}, \quad (18a)$$

$$\Pi_{xy}^* = -\sqrt{\frac{3}{2} \frac{\chi}{\psi} \left(1 - \frac{\chi}{\psi} \right)}, \quad (18b)$$

$$\dot{\gamma}^* = \sqrt{\frac{3}{2} \frac{\psi\chi}{1-\chi/\psi}}. \quad (18c)$$

Equation (18c) shows that the steady translational temperature scales quadratically with the shear rate. More explicitly,

$$T_t = T_t^0 \left(\frac{\dot{\gamma}}{\nu^0} \right)^2 \frac{2}{3} \frac{1-\chi/\psi}{\psi\chi}, \quad (19)$$

where T_t^0 is an arbitrary reference temperature and $\nu^0 \propto \sqrt{T_t^0}$ is the associated reference collision frequency.

Combining Eqs. (18a) and (18b), one obtains the nonequilibrium ‘‘equation of state’’

$$\Pi_{xy}^* = -\frac{1}{2} \sqrt{\frac{3}{2} \Pi_{xx}^* (2 - \Pi_{xx}^*)}, \quad (20)$$

which holds for arbitrary α , β , and κ , and coincides with that derived from a Bhatnagar–Gross–Krook-like model [35]. Analogously,

$$\frac{\dot{\gamma}^*}{\psi} = \sqrt{\frac{3}{2} \frac{\Pi_{xx}^*}{2 - \Pi_{xx}^*}}. \quad (21)$$

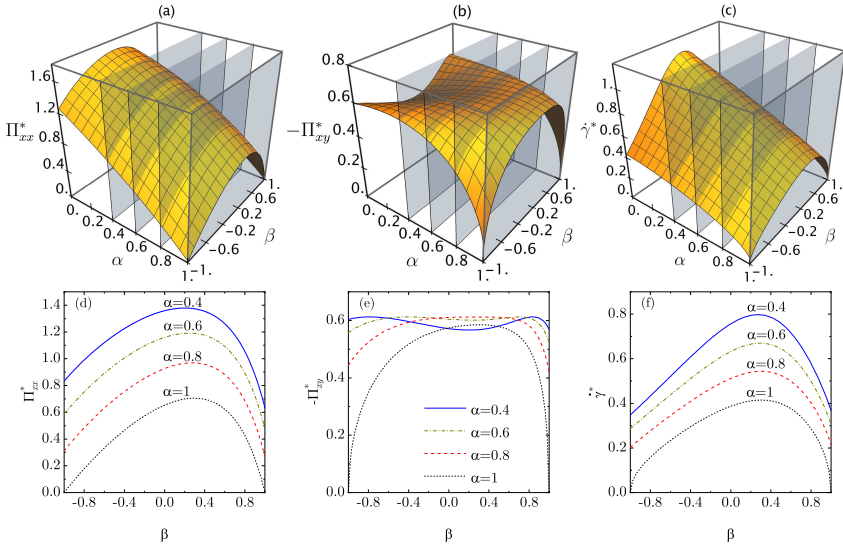


Fig. 2 Top panels: reduced normal stress Π_{xx}^* (a), reduced shear stress $-\Pi_{xy}^*$ (b), and reduced shear rate $\dot{\gamma}^*$ (c) as functions of the normal restitution coefficient α and the tangential restitution coefficient β for $\kappa = \frac{2}{5}$. The displayed planar surfaces correspond to $\alpha = 0.4, 0.6, 0.8$, and 1 . Bottom panels (d–f): corresponding cross-sections at fixed α .

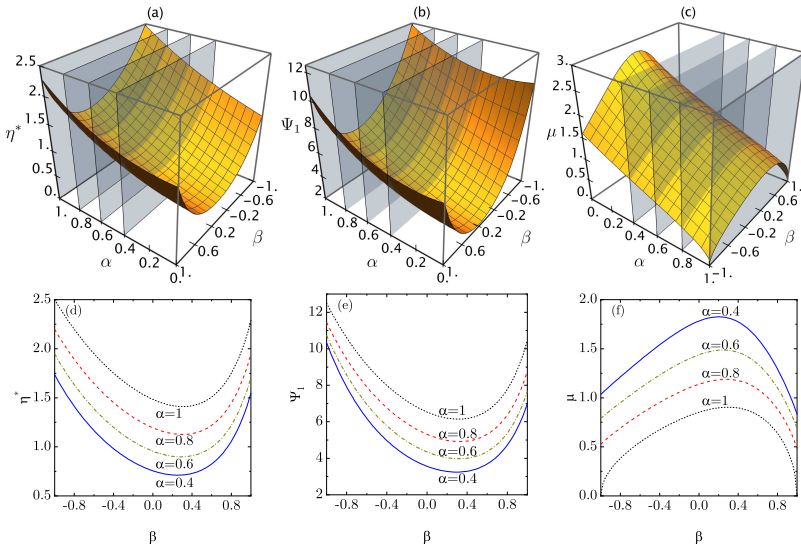


Fig. 3 Top panels: reduced shear viscosity η^* (a), first viscometric function Ψ_1 (b), and friction coefficient μ (c) as functions of the normal restitution coefficient α and the tangential restitution coefficient β for $\kappa = \frac{2}{5}$. The displayed planar surfaces correspond to $\alpha = 0.4, 0.6, 0.8$, and 1 . Bottom panels (d–f): corresponding cross-sections at fixed α .

Figure 2 shows the dependence of Π_{xx}^* , $-\Pi_{xy}^*$, and $\dot{\gamma}^*$ on α and β for uniform spheres, $\kappa = \frac{2}{5}$. At fixed α , both the reduced normal stress Π_{xx}^* and the reduced shear rate $\dot{\gamma}^*$ exhibit a nonmonotonic dependence on β , with a maximum around $\beta \sim 0-0.4$. At fixed β , Π_{xx}^* and $\dot{\gamma}^*$ increase monotonically as α decreases. The behavior of Π_{xy}^* is more intricate due to the combined dependence through χ and ψ .

To further characterize the rheology of the USF, we introduce the reduced non-Newtonian shear viscosity η^* , the first viscometric function Ψ_1 , and the friction coefficient μ [9], defined as

$$\eta^* \equiv -\frac{\Pi_{xy}^*}{\dot{\gamma}^*} = \frac{1 - \chi/\psi}{\psi} = \frac{2 - \Pi_{xx}^*}{2\psi}, \quad (22a)$$

$$\Psi_1 \equiv \frac{\Pi_{xx}^* - \Pi_{yy}^*}{\dot{\gamma}^{*2}} = 2\frac{1 - \chi/\psi}{\psi^2} = \frac{2 - \Pi_{xx}^*}{\psi^2}, \quad (22b)$$

$$\mu \equiv -\frac{\Pi_{xy}^*}{1 + \Pi_{yy}^*} = \sqrt{\frac{3}{2}} \frac{\chi/\psi}{1 - \chi/\psi} = \sqrt{\frac{3}{2}} \frac{\Pi_{xx}^*}{2 - \Pi_{xx}^*}. \quad (22c)$$

These quantities are plotted in Fig. 3 for $\kappa = \frac{2}{5}$. The shear viscosity and the first viscometric function increase with increasing α and display a nonmonotonic dependence on β , with a minimum in the region $\beta \sim 0-0.4$. The friction coefficient exhibits a qualitative dependence on α and β similar to that of the reduced shear rate.

The relatively large values of the first viscometric function highlight the strong non-Newtonian character of the USF. Moreover, the qualitative dependence of the USF shear viscosity on the coefficients of restitution is opposite to that of the Newtonian shear viscosity (compare Fig. 3(d) with Fig. 1(a) of Ref. [6]).

In the special case of inelastic and perfectly smooth particles ($\alpha < 1$, $\beta = -1$), the above expressions reduce to

$$\Pi_{xx}^* = 5\frac{1 - \alpha}{4 - \alpha}, \quad \Pi_{xy}^* = -\frac{3}{2}\sqrt{\frac{5}{2}}\frac{\sqrt{1 - \alpha^2}}{4 - \alpha}, \quad \dot{\gamma}^* = \sqrt{\frac{2}{5}}\frac{4 - \alpha}{6}\sqrt{1 - \alpha^2}, \quad (23a)$$

$$\eta^* = \frac{45}{2(4 - \alpha)^2}, \quad \Psi_1 = \frac{675}{(4 - \alpha)^3(1 + \alpha)}, \quad \mu = \sqrt{\frac{5}{2}}\frac{1 - \alpha}{1 + \alpha}. \quad (23b)$$

These results agree with those previously obtained for the IMM [21, 23].

In the opposite limit of elastic and perfectly rough particles ($\alpha = 1$, $\beta = 1$), one has $\Pi_{xx}^* = \Pi_{xy}^* = \dot{\gamma}^* = \mu = 0$ and

$$\eta^* = \frac{5}{2}(1 + \kappa)^2 \frac{3 + 10\kappa}{(1 + 5\kappa)(3 + 5\kappa)}, \quad \Psi_1 = 2\eta^{*2}. \quad (24)$$

In this case, η^* coincides with the Newtonian shear viscosity [6] of the Pidduck gas [40–44], while Ψ_1 represents a Burnett coefficient [44].

5 Conclusions

In this work we have derived exact results for the USF of a granular gas composed of inelastic and rough Maxwell particles. This study completes the program initiated in our previous papers [5, 6], where the collisional moments and the NSF transport coefficients of the IRMM were obtained exactly.

The mean-field character of the IRMM makes it possible to evaluate in closed form the collisional production rates of the second-degree moments and, consequently, to solve exactly the nonlinear rheological problem posed by the steady USF. As in the smooth Maxwell case, the structure of the moment equations allows for an exact determination of the reduced stress tensor and the reduced shear rate without recourse to approximate closures.

A number of remarkable features emerge. First, the rotational-to-translational temperature ratio $\theta = T_r/T_t$ is independent of the coefficient of normal restitution α and depends only on the tangential restitution β and the reduced moment of inertia κ . Moreover, the spin-spin tensor is strictly proportional to the stress tensor, with a proportionality factor that is also independent of α . Second, the nonlinear rheological functions—reduced normal stresses, reduced shear stress, shear rate, shear viscosity, viscometric function, and friction coefficient—are obtained in explicit form in terms of two effective parameters, χ and ψ , which generalize the cooling rate and the stress relaxation rate of the smooth model.

The dependence of the rheological properties on α and β is highly nontrivial. For uniform spheres ($\kappa = 2/5$), the reduced normal stress and the reduced shear rate exhibit a nonmonotonic dependence on β , with extrema at intermediate roughness, while they increase monotonically with increasing inelasticity (decreasing α). The first viscometric function attains relatively large values, clearly illustrating the strongly non-Newtonian character of the USF in the IRMM. Interestingly, the qualitative dependence of the nonlinear shear viscosity on the coefficients of restitution is opposite to that of the Newtonian shear viscosity derived previously.

In the limiting cases of perfectly smooth particles and of elastic perfectly rough particles, our results consistently reduce to the known solutions for the IMM and for the Pidduck IRMM gas, respectively. These reductions provide stringent consistency checks of the results.

Overall, the IRMM provides a rare example of a granular model where non-Newtonian rheology in a genuinely nonlinear state can be analyzed exactly in the presence of both inelasticity and roughness. The results reported here may serve as a benchmark for approximate kinetic theories and for numerical simulations of rough granular gases under shear.

Acknowledgments. A.S. acknowledges financial support from Grant No. PID2024-156352NB-I00 funded by MCIU/AEI/10.13039/501100011033 and by ERDF/EU, and from Grant No. GR24022 funded by the Junta de Extremadura (Spain).

Data availability. The datasets employed to generate Figs. 1–3 are available from the corresponding author on reasonable request.

Declarations

Conflict of interest. The authors declare no conflicts of interest that are relevant to the content of this article.

References

- [1] N.V. Brilliantov, T. Pöschel, *Kinetic Theory of Granular Gases* (Oxford University Press, Oxford, 2004)
- [2] V. Garzó, *Granular Gaseous Flows. A Kinetic Theory Approach to Granular Gaseous Flows* (Springer Nature, Switzerland, 2019)
- [3] A.V. Bobylev, J.A. Carrillo, I.M. Gamba, On some properties of kinetic and hydrodynamic equations for inelastic interactions. *J. Stat. Phys.* **98**, 743–773 (2000). <https://doi.org/10.1023/A:1018627625800>
- [4] J.T. Jenkins, M.W. Richman, Kinetic theory for plane flows of a dense gas of identical, rough, inelastic, circular disks. *Phys. Fluids* **28**, 3485–3494 (1985). <https://doi.org/10.1063/1.865302>
- [5] G.M. Kremer, A. Santos, Granular gas of inelastic and rough Maxwell particles. *J. Stat. Phys.* **189**, 23 (2022). <https://doi.org/10.1007/s10955-022-02984-6>
- [6] A. Santos, G.M. Kremer, Exact transport coefficients from the inelastic rough Maxwell model of a granular gas. *J. Stat. Phys.* **191**, 54 (2024). <https://doi.org/10.1007/s10955-024-03269-w>
- [7] A. Santos, V. Garzó, J.W. Dufty, Inherent rheology of a granular fluid in uniform shear flow. *Phys. Rev. E* **69**, 061,303 (2004). <https://doi.org/10.1103/PhysRevE.69.061303>
- [8] C.S. Campbell, A. Gong, The stress tensor in a two-dimensional granular shear flow. *J. Fluid Mech.* **164**, 107–125 (1986). <https://doi.org/10.1017/S0022112086002495>
- [9] C.S. Campbell, The stress tensor for simple shear flows of a granular material. *J. Fluid Mech.* **203**, 449–473 (1989). <https://doi.org/10.1017/S0022112089001540>
- [10] C.S. Campbell, Self-diffusion in granular shear flows. *J. Fluid Mech.* **348**, 85–101 (1997). <https://doi.org/10.1017/S0022112097006496>

- [11] J.M. Montanero, V. Garzó, M. Alam, S. Luding, Rheology of two- and three-dimensional granular mixtures under uniform shear flow: Enskog kinetic theory versus molecular dynamics simulations. *Granul. Matter* **8**, 103–115 (2006). <https://doi.org/10.1007/s10035-006-0001-7>
- [12] M.G. Chamorro, F. Vega Reyes, V. Garzó, Non-Newtonian hydrodynamics for a dilute granular suspension under uniform shear flow. *Phys. Rev. E* **92**, 052,205 (2015). <https://doi.org/10.1103/physreve.92.052205>
- [13] H. Hayakawa, S. Takada, V. Garzó, Kinetic theory of shear thickening for a moderately dense gas-solid suspension: From discontinuous thickening to continuous thickening. *Phys. Rev. E* **96**, 042,903 (2017). <https://doi.org/10.1103/PhysRevE.96.042903>
- [14] H. Hayakawa, S. Takada, Kinetic theory of discontinuous rheological phase transition for a dilute inertial suspension. *Prog. Theor. Exp. Phys.* **2019**, 083J01 (2019). <https://doi.org/10.1093/ptep/ptz075>
- [15] J.J. Brey, M.J. Ruiz-Montero, F. Moreno, Steady uniform shear flow in a low density granular gas. *Phys. Rev. E* **55**, 2846–2856 (1997). <https://doi.org/10.1103/PhysRevE.55.2846>
- [16] V. Garzó, Transport coefficients for an inelastic gas around uniform shear flow: Linear stability analysis. *Phys. Rev. E* **73**, 021,304 (2006). <https://doi.org/10.1103/PhysRevE.73.021304>
- [17] R. Gómez González, V. Garzó, Simple shear flow in granular suspensions: Inelastic Maxwell models and BGK-type kinetic model. *J. Stat. Mech.* **013206** (2019). <https://doi.org/10.1088/1742-5468/aaf719>
- [18] A. Astillero, A. Santos, Uniform shear flow in dissipative gases: Computer simulations of inelastic hard spheres and frictional elastic hard spheres. *Phys. Rev. E* **72**, 031,309 (2005). <https://doi.org/10.1103/PhysRevE.72.031309>
- [19] S. Takada, H. Hayakawa, A. Santos, V. Garzó, Enskog kinetic theory of rheology for a moderately dense inertial suspension. *Phys. Rev. E* **102**, 022,907 (2020). <https://doi.org/10.1103/PhysRevE.102.022907>
- [20] C. Cercignani, Shear flow of a granular material. *J. Stat. Phys.* **102**, 1407–1415 (2001). <https://doi.org/10.1023/A:1004804815471>
- [21] V. Garzó, Nonlinear transport in inelastic Maxwell mixtures under simple shear flow. *J. Stat. Phys.* **112**, 657–683 (2003). <https://doi.org/10.1023/A:1023828109434>

- [22] V. Garzó, Shear-rate dependent transport coefficients for inelastic Maxwell models. *J. Phys. A: Math. Theor.* **40**, 10,729–10,767 (2007). <https://doi.org/10.1088/1751-8113/40/35/002>
- [23] A. Santos, V. Garzó, Simple shear flow in inelastic Maxwell models. *J. Stat. Mech.* **P08021** (2007). <https://doi.org/10.1088/1742-5468/2007/08/P08021>
- [24] V. Garzó, Mass flux of a binary mixture of maxwell molecules under shear flow. *Physica A* **387**, 3423–3431 (2008). <https://doi.org/10.1016/j.physa.2008.02.019>
- [25] V. Garzó, E. Trizac, Rheological properties for inelastic Maxwell mixtures under shear flow. *J. Non-Newton. Fluid Mech.* **165**, 932–940 (2010). <https://doi.org/10.1016/j.jnnfm.2010.01.016>
- [26] V. Garzó, A. Santos, Hydrodynamics of inelastic Maxwell models. *Math. Model. Nat. Phenom.* **6**(4), 37–76 (2011). <https://doi.org/10.1051/mmnp/20116403>
- [27] V. Garzó, E. Trizac, Impurity in a sheared inelastic Maxwell gas. *Phys. Rev. E* **85**, 011,302 (2012). <https://doi.org/10.1103/PhysRevE.85.011302>
- [28] N. Khalil, V. Garzó, A. Santos, Hydrodynamic Burnett equations for inelastic Maxwell models of granular gases. *Phys. Rev. E* **89**, 052201 (2014). <https://doi.org/10.1103/PhysRevE.89.052201>
- [29] V. Garzó, E. Trizac, Generalized transport coefficients for inelastic Maxwell mixtures under shear flow. *Phys. Rev. E* **92**, 052,202 (2015). <https://doi.org/10.1103/PhysRevE.92.052202>
- [30] V. Garzó, N. Khalil, E. Trizac, Anomalous transport of impurities in inelastic Maxwell gases. *Eur. Phys. J. E* **38**, 16 (2015). <https://doi.org/10.1140/epje/i2015-15016-5>
- [31] V. Garzó, E. Trizac, Tracer diffusion coefficients in a sheared inelastic Maxwell gas. *J. Stat. Mech.* **073206** (2016). <https://doi.org/10.1088/1742-5468/2016/07/073206>
- [32] N. Khalil, V. Garzó, Unified hydrodynamic description for driven and undriven inelastic Maxwell mixtures at low density. *J. Phys. A: Math. Theor.* **53**, 355002 (2020). <https://doi.org/10.1088/1751-8121/ab9f72>
- [33] C. Sánchez Romero, V. Garzó, High-degree collisional moments of inelastic Maxwell mixtures—Application to the homogeneous cooling and uniform shear flow states. *Entropy* **25**, 222 (2023). <https://doi.org/10.3390/e25020222>

- [34] B. Gayen, M. Alam, Orientational correlation and velocity distributions in uniform shear flow of a dilute granular gas. *Phys. Rev. Lett.* **100**, 068,002 (2008). <https://doi.org/10.1103/PhysRevLett.100.068002>
- [35] A. Santos, A Bhatnagar–Gross–Krook-like model kinetic equation for a granular gas of inelastic rough hard spheres. *AIP Conf. Proc.* **1333**, 41–48 (2011). <https://doi.org/10.1063/1.3562623>
- [36] R. Gómez González, V. Garzó, Non-Newtonian rheology in inertial suspensions of inelastic rough hard spheres under simple shear flow. *Phys. Fluids* **32**, 073315 (2020). <https://doi.org/10.1063/5.0015241>
- [37] A. Santos, G.M. Kremer, V. Garzó, Energy production rates in fluid mixtures of inelastic rough hard spheres. *Prog. Theor. Phys. Suppl.* **184**, 31–48 (2010). <https://doi.org/10.1143/PTPS.184.31>
- [38] M. Babic, Average balance equations for granular materials. *Intl. J. Eng. Sci.* **35**, 523–548 (1997). [https://doi.org/10.1016/S0020-7225\(96\)00094-8](https://doi.org/10.1016/S0020-7225(96)00094-8)
- [39] N. Mitarai, H. Hayakawa, H. Nakanishi, Collisional granular flow as a micropolar fluid. *Phys. Rev. Lett.* **88**, 174301 (2002). <https://doi.org/10.1103/PhysRevLett.88.174301>
- [40] F.B. Pidduck, The kinetic theory of a special type of rigid molecule. *Proc. R. Soc. Lond. A* **101**, 101–112 (1922). <https://doi.org/10.1098/rspa.1922.0028>
- [41] D.W. Condiff, W. Lu, J.S. Dahler, Transport properties of polyatomic fluids, a dilute gas of perfectly rough spheres. *J. Chem. Phys.* **42**, 3445–3475 (1965). <https://doi.org/10.1063/1.1695749>
- [42] B.J. McCoy, S.I. Sandler, J.S. Dahler, Transport properties of polyatomic fluids. IV. The kinetic theory of a dense gas of perfectly rough spheres. *J. Chem. Phys.* **45**(10), 3485–3512 (1966). <https://doi.org/10.1063/1.1727365>
- [43] S. Chapman, T.G. Cowling, *The Mathematical Theory of Non-Uniform Gases*, 3rd edn. (Cambridge University Press, Cambridge, UK, 1970)
- [44] G.M. Kremer, *An Introduction to the Boltzmann Equation and Transport Processes in Gases* (Springer, Berlin, 2010)